Regime Shift in Arctic Ocean Sea-Ice Extent

Harry L. Stern[1]

[1]University of Washington Applied Physics Laboratory

January 12, 2025

Abstract

A regime shift is an abrupt, substantial, and persistent change in the state of a system. We show that a regime shift in the September Arctic sea-ice extent (SIE) occurred in 2007. Before 2007, September SIE was declining approximately linearly. In September 2007, SIE had its largest year-to-year drop (by a wide margin) in the entire 46-year satellite record (1979-2024). Since 2007, September SIE has been approximately constant, i.e., no long-term trend. The regime shift in 2007 was caused by significant export and melt of older and thicker sea ice over the previous 2 to 3 years, as documented in other studies. We test alternatives to the traditional linear model of declining September SIE, and discuss possible explanations for the lack of a trend since 2007.

Regime Shift in Arctic Ocean Sea-Ice Extent

Harry L. Stern[1]

[1]Polar Science Center, Applied Physics Laboratory, University of Washington, Seattle

Corresponding author: Harry L. Stern (hstern@uw.edu)

Key Points

A regime shift occurred in 2007 in the September Arctic sea-ice extent, from a downward trend (1979-2006) to no trend (2007-2024).

The period of no trend is inconsistent with a linear model of decline during 1979-2024, so an alternative description should be used.

Abstract

A regime shift is an abrupt, substantial, and persistent change in the state of a system. We show that a regime shift in the September Arctic sea-ice extent (SIE) occurred in 2007. Before 2007, September SIE was declining approximately linearly. In September 2007, SIE had its largest year-to-year drop (by a wide margin) in the entire 46-year satellite record (1979-2024). Since 2007, September SIE has been approximately constant, i.e., no long-term trend. The regime shift in 2007 was caused by significant export and melt of older and thicker sea ice over the previous

2 to 3 years, as documented in other studies. We test alternatives to the traditional linear model of declining September SIE, and discuss possible explanations for the lack of a trend since 2007.

Plain Language Summary

The Arctic Ocean freezes in winter and melts back in summer, but not completely – some sea ice always remains in the ocean at the end of the melt season in September. However, the area of that remaining sea ice has greatly declined since satellites began monitoring it in 1979. We show that the decline of September sea-ice area has not been steady over the years, as it is commonly portrayed. After declining from 1979 to 2006, there was a huge loss of sea ice in September 2007, followed by 18 years of ups and downs but no long-term trend. We say that a regime shift occurred in 2007 because the behavior of the September sea-ice area changed from declining to stable. We propose a simplified way of looking at the 46-year record of September sea-ice area, and we discuss possible explanations for the lack of a trend since 2007.

1. Introduction

Sea ice in the Arctic Ocean goes through an annual cycle of growth in winter and melt in summer. The area covered by sea ice in the Arctic Ocean has declined in all months of the year since the beginning of the satellite record in 1979, and its thickness has also declined (Fox-Kemper et al., 2021; Meier and Stroeve, 2022). Sumata et al. (2023) recently documented a regime shift in Arctic sea-ice thickness in 2007, from a thicker and more deformed ice cover to a thinner and more uniform ice cover. We show that a regime shift in Arctic sea-ice extent also occurred in 2007. A regime shift is an abrupt, substantial, and persistent change in the state of a system (Reid et al., 2015).

Sea-ice concentration (SIC) is the fraction of an area that is covered by sea ice. Gridded SIC data products are regularly produced from spaceborne passive microwave sensors with grid sizes ranging from 3.125 × 3.125 km (e.g. Spreen et al., 2008) to 25 × 25 km (e.g. DiGirolamo et al., 2022). Sea-ice extent (SIE) is defined as the total area of all grid cells with SIC greater than 15%.

Arctic SIE reaches its annual minimum in September. From 1979 to 2024, the linear trend in September SIE is -0.78×10^6 km^2 per decade (Figure 1) with standard deviation 0.058×10^6 km^2 per decade. The trend may also be expressed as −12.1% per decade (with standard deviation 0.9% per decade) relative to the mean September SIE of 6.4×10^6 km^2 as calculated over the 30-year base period 1981-2010 (Fetterer et al., 2017). However, we show that the September SIE abruptly changed behavior in 2007 from a downward trend to approximately constant in time.

2. Data

We use the monthly average September Arctic SIE from the Sea Ice Index produced by the National Snow and Ice Data Center (NSIDC) (Fetterer et al., 2017). The Sea Ice Index is derived from satellite passive microwave data (DiGirolamo et al., 2022) with grid size approximately 25 × 25 km. It is updated periodically to include the most recent satellite data. Values of September Arctic SIE for 1979-2024 are plotted in Figure 1.

We use the Sea Ice Index because the documentation states: “The … data are produced in a consistent way that makes the Index time-series appropriate for use when looking at long-term trends in sea ice cover.” (Fetterer et al., 2017).

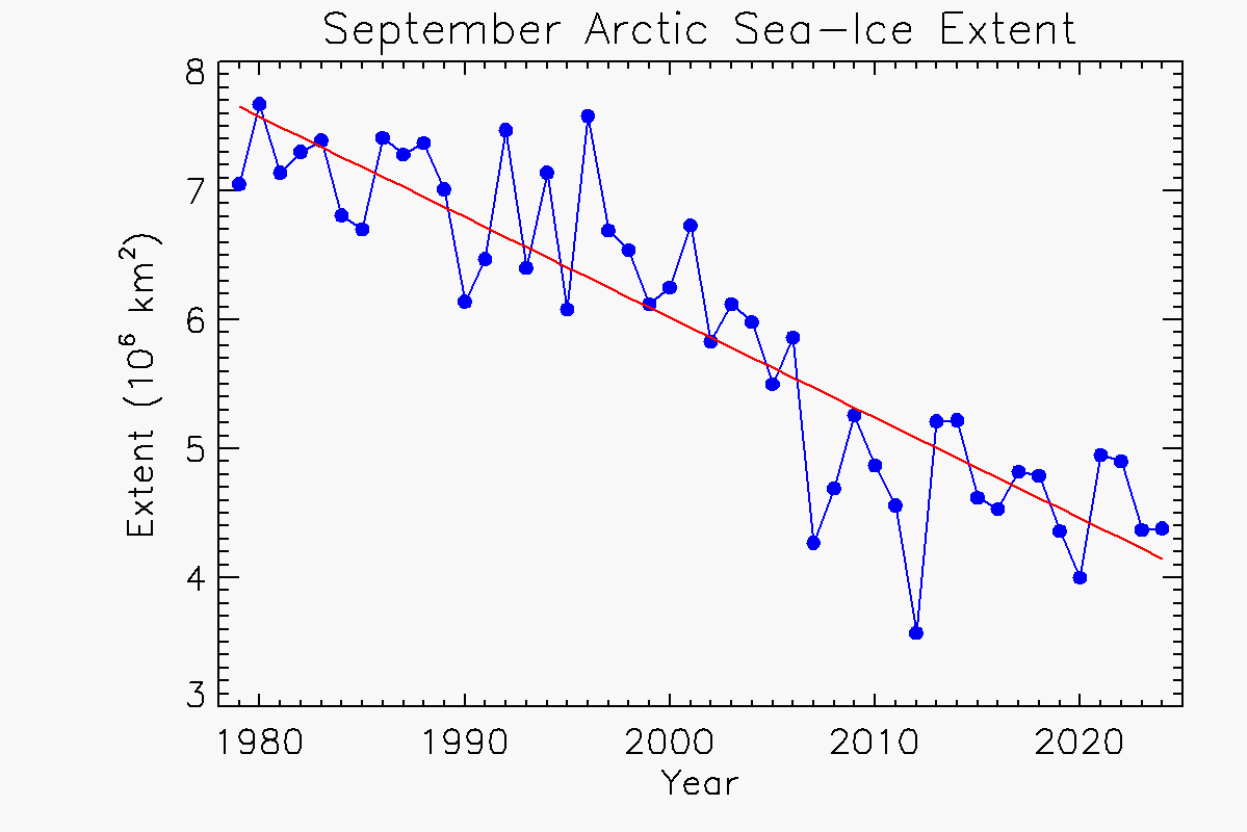

Figure 1. September Arctic sea-ice extent (blue dots, in units of 10^6 km^2) from the NSIDC Sea Ice Index (Fetterer et al., 2017). The linear least-squares fit is shown in red with slope −0.78 × 10^6 km^2 per decade.

3. Plausibility of a regime shift

Several factors point to the plausibility of a regime shift in the September SIE in 2007.

(i) As noted above, Sumata et al. (2023) found a regime shift in sea-ice thickness in 2007, from a thicker and more deformed ice cover to a thinner and more uniform ice cover. This opens the possibility of a change in the characteristic behavior of SIE as well, because a thinner ice cover is more susceptible to melt away by the end of summer (e.g., Lindsay and Zhang, 2005).

(ii) The largest year-to-year decline in September SIE occurred in 2007 with a loss of 1.6 $\times 10^6$ km^2 from the previous year. The next largest declines occurred in 1993 and 1995 with losses of 1.1 $\times 10^6$ km^2 from the previous year in both cases. Thus, the loss of area in 2007 was 45% greater than the next largest loss. In terms of percentage change from the previous year, the largest decline again occurred in 2007 with a drop of 27%. The next largest decline occurred in 2012, when a record-low SIE was set, with a drop of 22%. The declines in 1993 and 1995 were 14% and 15%, respectively. Thus, the percentage decline in 2007 again stands out as exceptional.

(iii) Consider partitioning the time series of September SIE into periods before and after a breakpoint T. Since there are 46 years in the time series, there are 45 possible breakpoints between years. For a given breakpoint T, find the minimum value of September SIE for the years before T (call it MIN), and the maximum value of September SIE for the years after T (call it MAX). Is it ever the case that MAX < MIN? The answer is yes, but only when T is between 2006 and 2007. That is the only breakpoint T in the time series for which all the values after T are less than all the values before T. This is illustrated in Figure 2 by the vertical and horizontal dotted lines. This indicates that the September SIE has never recovered from the jolt it received in 2007.

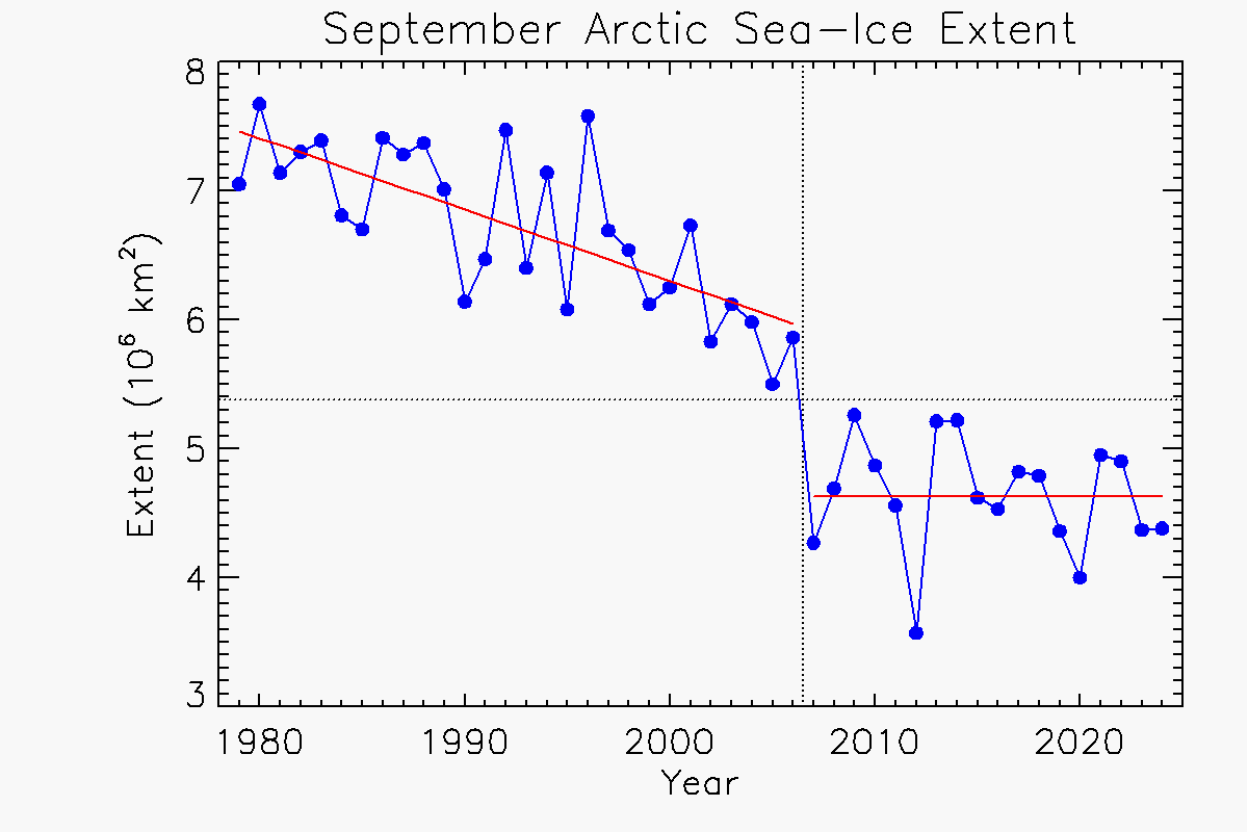

Figure 2. The same data as in Figure 1. The vertical dotted line between 2006 and 2007 marks the regime shift or breakpoint. The horizontal dotted line (at about 5.4×10^6 km^2) has the property that all the data values before the breakpoint are above the line and all the data values after the breakpoint are below the line. The only place in the time series where a horizontal line with that property can be drawn is for the breakpoint between 2006 and 2007. The linear least-squares fit for 1979-2006 is shown in red with slope -0.55×10^6 km^2 per decade. The mean sea-ice extent for 2007-2024 is also shown in red with value 4.63×10^6 km^2.

4. Detection of a regime shift

Rodionov (2004) presented an algorithm for detecting regime shifts in climate time series such as the Pacific Decadal Oscillation that have no long-term trend. The algorithm detects significant changes in the running mean of the time series using Student's t-test. The user must supply a parameter called the cut-off length, L, which is the minimum length of a regime. Although the algorithm is designed for time series with no long-term trend, Rodionov (2004) showed that it also works when a long-term trend is present (his Table 1). Sumata et al. (2023) used Rodionov's method for detecting a regime shift in sea-ice thickness, using a cut-off length of L = 7 years.

We first experimented with Rodionov's method on a time series of length 46 with values drawn from a normal distribution with zero mean and unit variance. We found that when the significance level of the t-test was set to p=0.05 the method detected spurious regime shifts for cut-off lengths $L \geq 7$, but when p=0.01 no such spurious regime shifts were detected. We therefore used p=0.01 in our application of the method to the September SIE time series.

We found that Rodionov's method detects a regime shift in the September SIE time series in 2007 for all values of the cut-off length L from 5 to 15 years. Additional regime shifts are also detected when $L \geq 9$ years. Note that in a time series with a long-term trend, as the cut-off length L increases, more and more of the running variability is in the trend as opposed to the fluctuations around the trend. For that reason, a shift in the running mean becomes more and more likely as L increases, which likely explains the additional regime shifts that are detected when $L \geq 9$ years.

Rodionov's method of regime shift detection depends on the significance level of the t-test and on the cut-off length L. It also assumes that the running variance of the time series, as calculated over segments of length L, does not change much over the entire time series. Although Rodionov's method does detect a regime shift in the September SIE in 2007, we would like to find a method that does not depend on tunable parameters and that tests the specific hypothesis of a regime shift in 2007 rather than searching for regime shifts in all possible years.

5. Bootstrap simulation

The full 46-year September SIE time series has a best-fit slope of $S_{46\text{-OBS}} = -0.78 \times 10^6$ km^2 per decade, and yet the last 18 years of the time series (2007-2024) has a best-fit slope of only $S_{18\text{-OBS}} = -0.099 \times 10^6$ km^2 per decade. Motivated by Figures 1 and 2 and the results of Sections 3 and 4, we want to determine how unusual that slope difference is. Specifically, we assume that the observed 46-year time series is well described by a linear model with slope $S_{46\text{-OBS}}$ plus residuals, and we ask how unusual it is for the final 18 years of that time series to have a best-fit slope of $S_{18\text{-OBS}}$. The null hypothesis (H_0) is that the observed slope $S_{18\text{-OBS}}$ is consistent with the 46-year linear model plus residuals. The alternative hypothesis (H_1) is that $S_{18\text{-OBS}}$ is not consistent with that model.

To test the hypotheses, we conduct a bootstrap simulation with the following general outline: Construct a large number of synthetic 46-year time series based on the same "linear model plus residuals" as the original time series; for each synthetic time series, calculate the slope of the final 18 years, creating a distribution of final 18-year slopes; compare the final 18-year slope of the original time series ($S_{18\text{-OBS}}$) to the distribution of synthetically derived slopes;

153 if $S_{18\text{-OBS}}$ lies in the outer 1% of the distribution, then reject H_0 and accept H_1; otherwise, do not
154 reject H_0.

155 The specific steps are as follows:

156 (i) Subtract the best-fit linear model of the 46-year September SIE time series (see Figure
157 1) from the time series itself to obtain residuals with zero mean.

158 (ii) Test whether the lag-1 autocorrelation of the residuals is significantly different from
159 zero or not, using the Durbin-Watson test (see Supporting Information, Text S1). The result is
160 that the lag-1 autocorrelation is not significantly different from zero, which means that the
161 bootstrap simulation does not need to account for autocorrelation in the residuals.

162 (iii) Randomly permute the order of the residuals and then add them back to the original
163 linear model to create a new (synthetic) time series. Calculate the best-fit slope for the full 46-
164 year synthetic time series (call it S_{46}) and the best-fit slope for the final 18 years (call it S_{18}).
165 Note that the slope S_{46} will be nearly the same as the slope of the original time series, but not
166 exactly the same, because the order of the residuals affects the least-squares fitting. For example,
167 a large anomaly near the middle of a time series has very little influence on the least-squares
168 slope, while the same anomaly at the end of the time series has a larger influence. For that
169 reason, S_{46} and S_{18} are both calculated and saved. Nevertheless, the synthetic time series has
170 nearly the same 46-year least-squares slope and residuals as the original time series. The real
171 quantity of interest is the slope of the final 18 years, S_{18}.

172 (iv) Repeat step (iii) 10,000 times to obtain a distribution of S_{18} and a distribution of S_{46}.
173 The resulting 10,000 pairs of numbers are plotted in Figure S1, with S_{18} on the X-axis and S_{46} on
174 the Y-axis.

175 The first point to note in Figure S1 is that the distribution of S_{46} is very narrow: its
176 standard deviation (0.057×10^6 km^2 per decade) is only 7% of the magnitude of its mean value
177 (0.78×10^6 km^2 per decade). This shows that most of the synthetic time series have nearly the
178 same least-squares slope as the original time series, and therefore nearly the same residuals (but
179 in a different order). Thus, the pool of 10,000 synthetic time series is representative of the
180 original time series for the purpose of the bootstrap simulation.

181 The second point to note in Figure S1 is that the observed value of the final 18-year slope
182 ($S_{18\text{-OBS}} = -0.099 \times 10^6$ km^2 per decade) is at the far extreme edge of the distribution of S_{18}: only
183 16 out of 10,000 values are larger than $S_{18\text{-OBS}}$. The standard deviation of S_{18} is 0.23×10^6 km^2
184 per decade, so $S_{18\text{-OBS}}$ exceeds the mean of S_{18} by 2.9 standard deviations. At the other end of the
185 distribution, only 13 out of 10,000 values are more than 2.9 standard deviations smaller than the
186 mean of S_{18}. Taken together, only 0.3% of the simulated slopes S_{18} are more extreme than the
187 observed value $S_{18\text{-OBS}}$. Therefore, we reject the null hypothesis and conclude that a linear model
188 is not appropriate for the 46-year time series of September SIE because the trend over the final
189 18 years is not consistent with such a model.

190

191 **6. Alternatives to the linear model**

192

193 In light of the results in the previous section, we consider several alternatives to a linear
194 model of September SIE: a piecewise-linear model with a breakpoint between 2006 and 2007, a
195 cubic polynomial, and a Gompertz model. Each alternative model contains four adjustable
196 parameters, so the models are directly comparable to one another. Since a linear model contains

only two adjustable parameters, the alternative models naturally provide better fits. A comparison of the models and their performance is given in Table 1.

The simplest piecewise-linear model of September SIE consists of a breakpoint between 2006 and 2007 and a linear fit on either side of the breakpoint. However, the slope of the best-fit line to the years 2007-2024 is $S_{18\text{-}OBS} = -0.099 \times 10^6$ km^2 per decade with standard deviation 0.20×10^6 km^2 per decade, which is statistically indistinguishable from zero, so a slope is unnecessary. The best-fit constant (in the least-squares sense) is the mean value, which is 4.6×10^6 km^2. The four parameters of the piecewise-linear model (shown in Figure 2) are then: the location of the breakpoint, the slope and intercept of the linear fit to the left of the breakpoint, and the constant fit (the mean) to the right of the breakpoint. This model is very simple to understand and interpret: September SIE declined approximately linearly for the first 28 years, then an unprecedented jolt hit in 2007 from which the SIE has never recovered. There has been no long-term trend since that time.

The cubic polynomial model (shown in Figure S2) is continuous – there is no breakpoint or jump in value. The idea is to see if a higher-order function can smoothly account for the large drop in September SIE in 2007, followed by a period of no long-term trend. One drawback of this model is the difficulty of explaining why the September SIE should evolve according to a cubic function of time.

The Gompertz function was invented to model human mortality and has been used to model the growth of animal populations, bacterial cells, and tumors (Gompertz function, 2024). It has also been used to model the September SIE (Stroeve et al., 2014; Hamilton, 2015). The Gompertz function has a sigmoid shape with slow growth (or decay) at the beginning and end, and faster growth (or decay) in the middle. The idea of using this model is to see if the faster

220 decay can be aligned with the drop in SIE in 2007, and the asymptotic value as $t \rightarrow \infty$ matched
221 with the mean SIE during 2007-2024. Details of the Gompertz model are in the Supporting
222 Information, Text S2 and Figure S2.

223 Of the three alternative models considered here, the one with a discontinuity in 2007
224 performs the best (Table 1). This lends further weight to the idea of a regime shift in 2007.

225

226

227

228 **Table 1.** Comparison of different models of the September sea-ice extent (SIE). The root-mean-
229 square (RMS) value of the residuals (fourth column) is in units of 10^6 km^2. The fraction of the
230 variance of the SIE that is explained by the model is given in the fifth column.

231

Model	**Continuous?**	**Number of parameters**	**RMS of residuals**	**Fraction of variance**
Linear	Yes	2	0.51	0.80
Piecewise-linear	No	4	0.41	0.87
Cubic	Yes	4	0.46	0.84
Gompertz	Yes	4	0.45	0.85

232

7. Discussion

We have shown that the September Arctic SIE underwent an abrupt, substantial, and persistent change in 2007, meeting the definition of a regime shift given by Reid et al. (2015). Before 2007, September SIE was declining approximately linearly. In September 2007, SIE had its largest year-to-year drop (by a wide margin) in the entire 46-year satellite record (1979-2024). Since 2007, September SIE has been approximately constant, i.e., no long-term trend.

The statistical evidence for a regime shift presented here calls for an explanation in terms of physical processes. While it is beyond the scope of the present work to conduct such process studies, e.g. with climate models, we can look to previous studies for insight. In the following, we consider the three segments of the September SIE time series: the decline (1979-2006), the extreme drop (2007), and the period of no long-term trend (2007-2024).

The decline of September SIE through 2006 was well documented at the time in observations and models (e.g., Lemke et al., 2007), although the models tended to underestimate the downward trend (Stroeve et al., 2007). More recently, Meehl et al. (2018) noted that the linear rate of decline of Arctic SIE was steeper during 2000-2014 than during 1979-1999. Their explanation is that "a combination of decadally varying tropical sea surface temperatures in the Pacific and Atlantic drove seasonally dependent patterns of stronger surface winds and sea ice drifts over the Arctic that produced accelerated decreases of Arctic sea ice concentrations after 2000." We note that their later period (2000-2014) spans the huge drop in September SIE in 2007 that initiated the regime shift, as well as the record-low September SIE in 2012. Their results are not inconsistent with ours because the trend in September SIE during 2000-2006 is about the same as during 1979-2000. Their steeper slope during 2000-2014 is due to the low values of SIE

from 2007 onward. In any case, the physical reason for the downward trend in Arctic SIE has been confidently attributed to global warming caused by anthropogenic greenhouse gas emissions (Fox-Kemper et al., 2021). Notz and Stroeve (2016) found that Arctic sea-ice loss is linearly related to anthropogenic CO_2 emissions.

The physical basis for a regime shift in 2007 is explained by Sumata et al. (2023) in reference to the sea-ice thickness: "The timing of the shift was preceded by a two-step reduction in residence time of sea ice in the Arctic Basin, initiated first in 2005 and followed by 2007." And then, "After the shift, the fraction of thick and deformed ice dropped by half and has not recovered to date." Similar conclusions about sea-ice loss were reached by Babb et al. (2023): the loss of multiyear ice (MYI) from the Arctic Ocean primarily occurred through stepwise reductions in 1989 and in 2006-2008; the reduction in 2006-2008 was the result of high MYI export and melt, and limited MYI replenishment. Maslanik et al. (2007) were the first to comment on the record-low SIE in 2007, also tying it to reduced MYI as well as ice transport: "Ice coverage in summer 2007 reached a record minimum, with ice extent declining by 42% compared to conditions in the 1980s. The much-reduced extent of the oldest and thickest ice, in combination with other factors such as ice transport that assist the ice-albedo feedback by exposing more open water, help explain this large and abrupt ice loss." The increase in the drift speed of Arctic sea ice (Rampal et al., 2009) also factored into the explanation given by Nghiem et al. (2007) for the significant reduction in perennial sea ice between March 2005 and March 2007. They found that a contributing mechanism was "ice loading into the Transpolar Drift (TD) together with an acceleration of the TD carrying excessive ice out of Fram Strait." For overviews of the 2007 SIE minimum, see Stroeve et al. (2008) and Zhang et al. (2008). The above observations clearly tie the record-low (at the time) SIE in September 2007 to the loss of MYI

279 through export. This led to a regime shift in the sea-ice thickness (Sumata et al., 2023) and (we
280 contend) a regime shift in the September SIE as well. In addition, Livina and Lenton (2013)
281 found an abrupt and persistent increase in the amplitude of the seasonal cycle of sea ice starting
282 in 2007, which they termed a tipping point. This is further evidence that 2007 was a pivotal year
283 for Arctic sea ice.

284 The period of no long-term trend in the September SIE (2007-2024) has been noted by
285 other researchers. Meier and Stroeve (2022) wrote: "The Arctic sea ice cover has undergone
286 substantial changes in the past 40+ years, including decline in areal extent in all months
287 (strongest during summer), thinning, loss of multiyear ice cover, earlier melt onset and ice
288 retreat, and later freeze-up and ice advance. In the past 10 years, these trends have been further
289 reinforced, though the trends (not statistically significant at $p<0.05$) in some parameters (e.g.,
290 extent) over the past decade are more moderate." In other words, they recognized that the trend
291 in Arctic SIE during approximately 2010-2020 was not significantly different from zero, but they
292 did not go so far as to call it a regime shift.

293 The fact that September Arctic SIE shows no trend during 2007-2024 may at first seem
294 hard to explain. The Earth continues to warm, and the Arctic is warming faster than the global
295 average (IPCC, 2021). One possibility is that the recent period of no trend is just interdecadal
296 variability. Baxter et al. (2019) found that "observational and model evidence shows that the
297 changes in summer sea ice since the 2000s reflect a continuous anthropogenically forced melting
298 masked by interdecadal variability of Arctic atmospheric circulation. This variation is partially
299 driven by teleconnections originating from sea surface temperature (SST) changes in the east-
300 central tropical Pacific" and this "has contributed to accelerated warming and Arctic sea ice loss
301 from 2007 to 2012, followed by slower declines in recent years, resulting in the appearance of a

slowdown over the past 11 years." In other words, they argue that the appearance of a slowdown in the decline of Arctic SIE since 2007 is due to interdecadal variability of Arctic atmospheric circulation.

As noted above, Sumata et al. (2023) found that after the regime shift of 2007, "the fraction of thick and deformed ice dropped by half and has not recovered to date." The variance of the sea-ice thickness also dropped abruptly in 2007 and has not recovered (their Figure 2), signaling the transition to a more uniform ice cover. With the Arctic Ocean thus dominated by first-year ice (confirmed also by Kwok, 2018), the SIE at the end of the summer melt season would be dominated by the production, melt, and export of first-year ice since the previous fall. Therefore, the September SIE during 2007-2024 may simply reflect the mean and year-to-year variability of first-year ice in a steady state (Figure 2). The Arctic Oscillation index, a climate index that characterizes the large-scale atmospheric circulation over the Arctic, has been in a positive phase since mid-2011 (NOAA Climate Prediction Center, 2024), which indicates lower than average air pressure over the Arctic (NOAA Climate.gov, 2024), driving a cyclonic circulation pattern in the Arctic Ocean with a lag of about one year (Morison et al., 2021). The persistence of this cyclonic mode in the ocean may be contributing to the steady state of the September SIE. This is similar to the argument made in the previous paragraph that the lack of trend in September SIE is due to interdecadal variability of Arctic atmospheric circulation.

Lindsay and Zhang (2005) proposed a three-stage framework for understanding the record or near-record lows in summer SIE in the years 2002-2005 that is partially applicable to 2007 and beyond. First, the sea ice was "pre-conditioned" through a gradual reduction in thickness during the late 1980s and 1990s. Second, a temporary change in atmospheric circulation embodied in two climate indexes, the Arctic Oscillation and the Pacific Decadal

Oscillation, provided the "trigger" that caused older, thicker sea ice to be flushed out the Arctic basin, resulting in an increase in the summer open water extent. Third, the positive ice-albedo feedback perpetuated and amplified the shift toward more summer open water and thinner ice. The feedback continued to drive the thinning of the sea ice even after the climate indexes returned to near-normal values in the late 1990s. The first and second stages of this framework apply equally well to the September SIE through 2007. The pre-conditioning stage was the thinning and areal reduction of 1979-2006. The trigger was the huge decline in 2007 caused by the export of ice from the Arctic basin. But annual declines have not been sustained (on average) in the post-2007 period, suggesting that the ice-albedo feedback has not been dominating the evolution of the ice cover.

Whatever the reason for the near-zero trend during 2007-2024, Arctic SIE is predicted to continue declining due to increasing global average air temperature caused by anthropogenic greenhouse gas emissions (Fox-Kemper et al., 2021). Based on global climate models, there is "*high confidence* that the Arctic Ocean will *likely* become practically sea ice free in the September mean for the first time … before the year 2050" in all emissions scenarios (Fox-Kemper et al., 2021). Thus, we would expect to see either a resumption of a steady decline in September SIE or a step-wise reduction through regime shifts facilitated by a younger and thinner ice pack that is more sensitive to external atmospheric forcing, whose decadal variability may also play a role.

Data availability

The data in Fetterer et al. (2017) are available from https://doi.org/10.7265/N5K072F8

An alternate URL is https://nsidc.org/data/g02135/versions/3

A direct link to September Arctic SIE data is:

https://noaadata.apps.nsidc.org/NOAA/G02135/north/monthly/data/N_09_extent_v3.0.csv

Acknowledgements

The author thanks Axel Schweiger, Ron Lindsay, and Jamie Morison for helpful comments and discussion. Funding was provided by NASA Interdisciplinary Research Grant 80NSSC20K1253.

References

Babb, D. G., Galley, R. J., Kirillov, S., Landy, J. C., Howell, S. E. L., Stroeve, J. C., et al. (2023). The stepwise reduction of multiyear sea ice area in the Arctic Ocean since 1980. *Journal of Geophysical Research: Oceans*,128, e2023JC020157. https://doi.org/10.1029/2023JC020157

Baxter, I., Q. Ding, A. Schweiger, M. L'Heureux, S. Baxter, T. Wang, Q. Zhang, K. Harnos, B. Markle, D. Topal, and J. Lu (2019). How Tropical Pacific Surface Cooling Contributed to Accelerated Sea Ice Melt from 2007 to 2012 as Ice Is Thinned by Anthropogenic Forcing, *Journal of Climate*, 32, 8583-8602, DOI: 10.1175/JCLI-D-18-0783.1

DiGirolamo, N., Parkinson, C. L., Cavalieri, D. J., Gloersen, P. & Zwally, H. J. (2022). Sea Ice Concentrations from Nimbus-7 SMMR and DMSP SSM/I-SSMIS Passive Microwave Data. (NSIDC-0051, Version 2). Boulder, Colorado USA. NASA National Snow and Ice Data Center Distributed Active Archive Center. https://doi.org/10.5067/MPYG15WAA4WX.

Fetterer, F., Knowles, K., Meier, W. N., Savoie, M. & Windnagel, A. K. (2017). Sea Ice Index. (G02135, Version 3). Boulder, Colorado USA. National Snow and Ice Data Center. https://doi.org/10.7265/N5K072F8. Date Accessed 11-10-2024.
Alternate URL: https://nsidc.org/data/g02135/versions/3

Fox-Kemper, B., H.T. Hewitt, C. Xiao, G. Aðalgeirsdóttir, S.S. Drijfhout, T.L. Edwards, N.R. Golledge, M. Hemer, R.E. Kopp, G. Krinner, A. Mix, D. Notz, S. Nowicki, I.S. Nurhati, L. Ruiz, J.-B. Sallée, A.B.A. Slangen, and Y. Yu (2021). Ocean, Cryosphere and Sea Level Change. In Climate Change 2021: The Physical Science Basis. Contribution of Working Group I to the Sixth Assessment Report of the Intergovernmental Panel on Climate Change [Masson-Delmotte, V., P. Zhai, A. Pirani, S.L. Connors, C. Péan, S. Berger, N. Caud, Y. Chen, L. Goldfarb, M.I. Gomis, M. Huang, K. Leitzell, E. Lonnoy, J.B.R. Matthews, T.K. Maycock, T. Waterfield, O. Yelekçi, R. Yu, and B. Zhou (eds.)]. Cambridge University Press, Cambridge, United Kingdom and New York, NY, USA, pp. 1211–1362, doi:10.1017/9781009157896.011.

Gompertz function (2024). Wikipedia, https://en.wikipedia.org/wiki/Gompertz_function
When accessed on 12/11/2024, this page was last edited on 8/13/2024 at 08:30 (UTC).

Hamilton, L. (2015). Pan-Arctic Outlook, contribution to the *Sea Ice Outlook: 2015 June Report*, Sea Ice Prediction Network, Arctic Research Consortium of the United States, https://www.arcus.org/sipn/sea-ice-outlook/2015/june

IPCC (2021). Summary for Policymakers. In: Climate Change 2021: The Physical Science Basis. Contribution of Working Group I to the Sixth Assessment Report of the Intergovernmental Panel on Climate Change [Masson-Delmotte, V., P. Zhai, A. Pirani, S. L. Connors, C. Péan, S. Berger, N. Caud, Y. Chen, L. Goldfarb, M. I. Gomis, M. Huang, K. Leitzell, E. Lonnoy, J. B. R. Matthews, T. K. Maycock, T. Waterfield, O. Yelekçi, R. Yu and B. Zhou (eds.)]. Cambridge University Press.

Kwok, R. (2018). Arctic sea ice thickness, volume, and multiyear ice coverage: losses and coupled variability (1958–2018), *Environ. Res. Lett.,* 13, 105005, https://doi.org/10.1088/1748-9326/aae3ec

Lemke, P., J. Ren, R.B. Alley, I. Allison, J. Carrasco, G. Flato, Y. Fujii, G. Kaser, P. Mote, R.H. Thomas and T. Zhang (2007). Observations: Changes in Snow, Ice and Frozen Ground. In: Climate Change 2007: The Physical Science Basis. Contribution of Working Group I to the Fourth Assessment Report of the Intergovernmental Panel on Climate Change [Solomon, S., D. Qin, M. Manning, Z. Chen, M. Marquis, K.B. Averyt, M. Tignor and H.L. Miller (eds.)]. Cambridge University Press, Cambridge, United Kingdom and New York, NY, USA.

414 Lindsay, R. W., and J. Zhang (2005). The Thinning of Arctic Sea Ice, 1988–2003: Have We
415 Passed a Tipping Point? *Journal of Climate*, 18, 4879-4894.
416
417 Livina, V. N., and T. M. Lenton (2013). A recent tipping point in the Arctic sea-ice cover: abrupt
418 and persistent increase in the seasonal cycle since 2007, *The Cryosphere*, 7, 275–286,
419 doi:10.5194/tc-7-275-2013
420
421 Maslanik, J. A., C. Fowler, J. Stroeve, S. Drobot, J. Zwally, D. Yi, and W. Emery (2007), A
422 younger, thinner Arctic ice cover: Increased potential for rapid, extensive sea-ice loss, *Geophys.*
423 *Res. Lett., 34,* L24501, doi:10.1029/2007GL032043.
424
425 Meehl, G. A., Chung, C. T. Y., Arblaster, J. M., Holland, M. M., & Bitz, C. M. (2018). Tropical
426 decadal variability and the rate of Arctic sea ice decrease. *Geophysical Research Letters*, 45,
427 11,326–11,333. https://doi.org/10.1029/2018GL079989
428
429 Meier, W.N., and J. Stroeve (2022). An updated assessment of the changing Arctic sea ice cover.
430 *Oceanography*, https://doi.org/10.5670/oceanog.2022.114.
431
432 Morison, J., R. Kwok, S. Dickinson, R. Andersen, C. Peralta-Ferriz, D. Morison, I. Rigor, S.
433 Dewey, and J. Guthrie (2021). The Cyclonic Mode of Arctic Ocean Circulation, *Journal of*
434 *Physical Oceanography*, 51, 1053-1075, DOI: 10.1175/JPO-D-20-0190.1
435

436 Nghiem, S. V., I. G. Rigor, D. K. Perovich, P. Clemente-Colon, J. W. Weatherly, and G. Neumann
437 (2007), Rapid reduction of Arctic perennial sea ice, *Geophys. Res. Lett.,* 34, L19504,
438 doi:10.1029/2007GL031138.
439
440 NOAA Climate.gov (2024). Climate Variability: Arctic Oscillation,
441 https://www.climate.gov/news-features/understanding-climate/climate-variability-arctic-
442 oscillation, accessed 12/24/2024.
443
444 NOAA Climate Prediction Center (2024). Standardized 3-Month Running Mean AO Index
445 Through November 2024,
446 https://www.cpc.ncep.noaa.gov/products/precip/CWlink/daily_ao_index/month_ao_index.shtml
447 Accessed 12/24/2024.
448
449 Notz, D. and J. Stroeve (2016). Observed Arctic sea-ice loss directly follows anthropogenic CO2
450 emission, *Science*, Vol 354, Issue 6313, pp. 747-750, DOI: 10.1126/science.aag2345
451
452 Rampal, P., J. Weiss, and D. Marsan (2009), Positive trend in the mean speed and deformation
453 rate of Arctic sea ice, 1979–2007, *J. Geophys. Res.,* 114, C05013, doi:10.1029/2008JC005066.
454
455 Reid, P.C., R.E. Hari, G. Beaugrand, D.M. Livingstone, C. Marty, D. Straile, J. Barichivich, E.
456 Goberville, R. Adriani, Y. Aono, R. Brown, J. Foster, P. Groisman, P. Helaouet, H. Hsu, R. Kirby,
457 J. Knight, A. Kraberg, J. Li, T-T Lo, R.A. Myneni, R.P. North, J.A. Pounds, T. Sparks, R. Stubi,

458 Y. Tian, K.H. Wiltshire, D. Xiao, and Z. Zhu (2015). Global impacts of the 1980s regime shift,
459 *Global Change Biology*, doi: 10.1111/gcb.13106
460
461 Rodionov, S.N. (2004). A sequential algorithm for testing climate regime shifts, *Geophysical*
462 *Research Letters*, 31, L09204, doi:10.1029/2004GL019448
463
464 Savin, N.E. and White, K.J. (1977). The Durbin-Watson Test for Serial Correlation with Extreme
465 Sample Sizes or Many Regressors. *Econometric*, 45, 1989-1996.
466 http://dx.doi.org/10.2307/1914122
467
468 Spreen, G., L. Kaleschke, and G.Heygster (2008). Sea ice remote sensing using AMSR-E 89
469 GHz channels, *J. Geophys. Res.*, 113, C02S03, doi:10.1029/2005JC003384.
470
471 Stroeve, J., M. M. Holland, W. Meier, T. Scambos, and M. Serreze (2007). Arctic sea ice
472 decline: Faster than forecast, *Geophys. Res. Lett.,* 34, L09501, doi:10.1029/2007GL029703.
473
474 Stroeve, J., M. Serreze, S. Drobot, S. Gearheard, M. Holland, J. Maslanik, W. Meier, and T.
475 Scambos (2008). Arctic Sea Ice Extent Plummets in 2007, *Eos Transactions*, Vol. 89, No. 2, pp.
476 13-20.
477
478 Stroeve, J., L. C. Hamilton, C. M. Bitz, and E. Blanchard-Wrigglesworth (2014). Predicting
479 September sea ice: Ensemble skill of the SEARCH Sea Ice Outlook 2008–2013, *Geophys. Res.*
480 *Lett.*, 41, 2411–2418, doi:10.1002/2014GL059388.

Sumata, Hiroshi, Laura de Steur, Dmitry V. Divine, Mats A. Granskog and Sebastian Gerland (2023). Regime shift in Arctic Ocean sea ice thickness, *Nature*, vol. 615, 443-449 https://doi.org/10.1038/s41586-022-05686-x

Zhang, J., R. Lindsay, M. Steele, and A. Schweiger (2008). What drove the dramatic retreat of arctic sea ice during summer 2007?, *Geophys. Res. Lett.,* 35, L11505, doi:10.1029/2008GL034005.

Regime Shift in Arctic Ocean Sea-Ice Extent

Harry L. Stern[1]

[1]Polar Science Center, Applied Physics Laboratory, University of Washington, Seattle

Corresponding author: Harry L. Stern (hstern@uw.edu)

Key Points

A regime shift occurred in 2007 in the September Arctic sea-ice extent, from a downward trend (1979-2006) to no trend (2007-2024).

The period of no trend is inconsistent with a linear model of decline during 1979-2024, so an alternative description should be used.

Abstract

A regime shift is an abrupt, substantial, and persistent change in the state of a system. We show that a regime shift in the September Arctic sea-ice extent (SIE) occurred in 2007. Before 2007, September SIE was declining approximately linearly. In September 2007, SIE had its largest year-to-year drop (by a wide margin) in the entire 46-year satellite record (1979-2024). Since 2007, September SIE has been approximately constant, i.e., no long-term trend. The regime shift in 2007 was caused by significant export and melt of older and thicker sea ice over the previous

2 to 3 years, as documented in other studies. We test alternatives to the traditional linear model of declining September SIE, and discuss possible explanations for the lack of a trend since 2007.

Plain Language Summary

The Arctic Ocean freezes in winter and melts back in summer, but not completely – some sea ice always remains in the ocean at the end of the melt season in September. However, the area of that remaining sea ice has greatly declined since satellites began monitoring it in 1979. We show that the decline of September sea-ice area has not been steady over the years, as it is commonly portrayed. After declining from 1979 to 2006, there was a huge loss of sea ice in September 2007, followed by 18 years of ups and downs but no long-term trend. We say that a regime shift occurred in 2007 because the behavior of the September sea-ice area changed from declining to stable. We propose a simplified way of looking at the 46-year record of September sea-ice area, and we discuss possible explanations for the lack of a trend since 2007.

1. Introduction

Sea ice in the Arctic Ocean goes through an annual cycle of growth in winter and melt in summer. The area covered by sea ice in the Arctic Ocean has declined in all months of the year since the beginning of the satellite record in 1979, and its thickness has also declined (Fox-Kemper et al., 2021; Meier and Stroeve, 2022). Sumata et al. (2023) recently documented a regime shift in Arctic sea-ice thickness in 2007, from a thicker and more deformed ice cover to a thinner and more uniform ice cover. We show that a regime shift in Arctic sea-ice extent also occurred in 2007. A regime shift is an abrupt, substantial, and persistent change in the state of a system (Reid et al., 2015).

Sea-ice concentration (SIC) is the fraction of an area that is covered by sea ice. Gridded SIC data products are regularly produced from spaceborne passive microwave sensors with grid sizes ranging from 3.125 × 3.125 km (e.g. Spreen et al., 2008) to 25 × 25 km (e.g. DiGirolamo et al., 2022). Sea-ice extent (SIE) is defined as the total area of all grid cells with SIC greater than 15%.

Arctic SIE reaches its annual minimum in September. From 1979 to 2024, the linear trend in September SIE is -0.78×10^6 km^2 per decade (Figure 1) with standard deviation 0.058×10^6 km^2 per decade. The trend may also be expressed as −12.1% per decade (with standard deviation 0.9% per decade) relative to the mean September SIE of 6.4×10^6 km^2 as calculated over the 30-year base period 1981-2010 (Fetterer et al., 2017). However, we show that the September SIE abruptly changed behavior in 2007 from a downward trend to approximately constant in time.

2. Data

We use the monthly average September Arctic SIE from the Sea Ice Index produced by the National Snow and Ice Data Center (NSIDC) (Fetterer et al., 2017). The Sea Ice Index is derived from satellite passive microwave data (DiGirolamo et al., 2022) with grid size approximately 25 × 25 km. It is updated periodically to include the most recent satellite data. Values of September Arctic SIE for 1979-2024 are plotted in Figure 1.

We use the Sea Ice Index because the documentation states: “The … data are produced in a consistent way that makes the Index time-series appropriate for use when looking at long-term trends in sea ice cover.” (Fetterer et al., 2017).

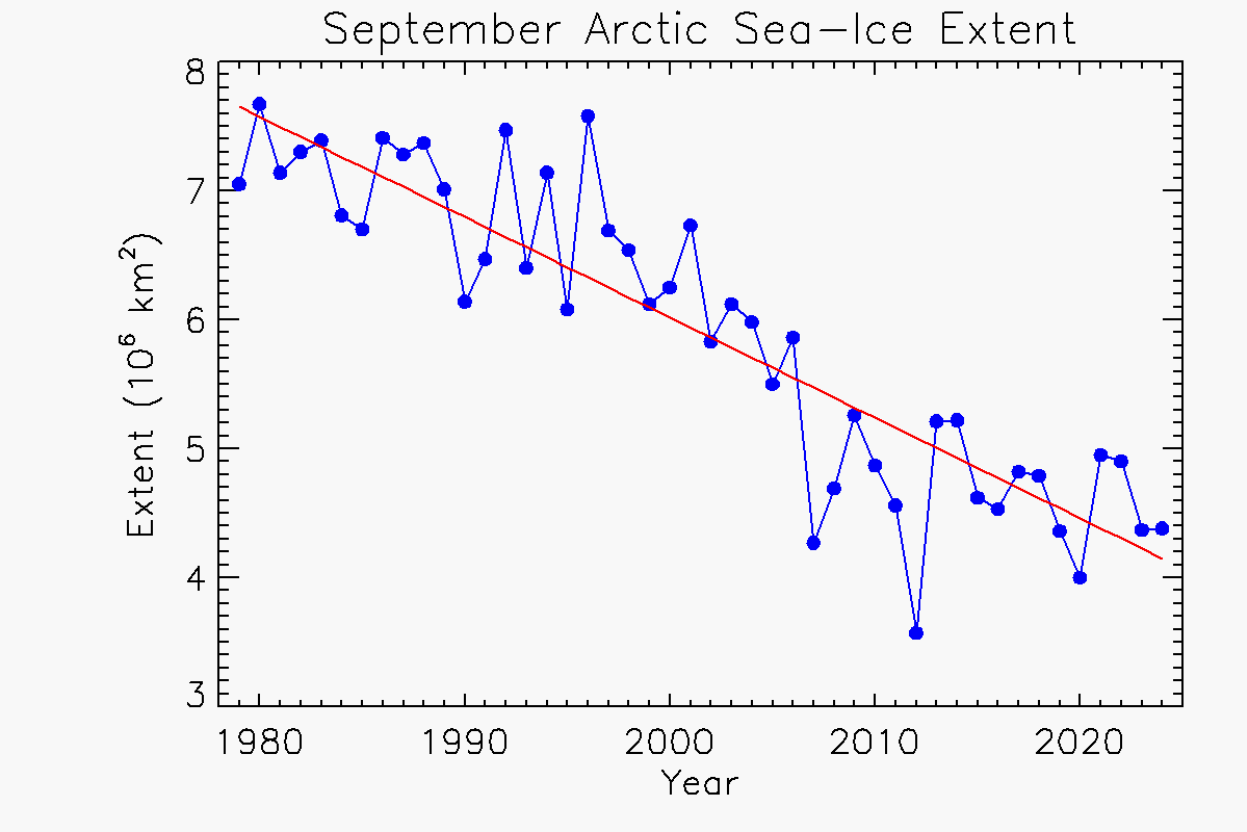

Figure 1. September Arctic sea-ice extent (blue dots, in units of 10^6 km^2) from the NSIDC Sea Ice Index (Fetterer et al., 2017). The linear least-squares fit is shown in red with slope −0.78 × 10^6 km^2 per decade.

3. Plausibility of a regime shift

Several factors point to the plausibility of a regime shift in the September SIE in 2007.

(i) As noted above, Sumata et al. (2023) found a regime shift in sea-ice thickness in 2007, from a thicker and more deformed ice cover to a thinner and more uniform ice cover. This opens the possibility of a change in the characteristic behavior of SIE as well, because a thinner ice cover is more susceptible to melt away by the end of summer (e.g., Lindsay and Zhang, 2005).

(ii) The largest year-to-year decline in September SIE occurred in 2007 with a loss of 1.6 $\times 10^6$ km^2 from the previous year. The next largest declines occurred in 1993 and 1995 with losses of 1.1 $\times 10^6$ km^2 from the previous year in both cases. Thus, the loss of area in 2007 was 45% greater than the next largest loss. In terms of percentage change from the previous year, the largest decline again occurred in 2007 with a drop of 27%. The next largest decline occurred in 2012, when a record-low SIE was set, with a drop of 22%. The declines in 1993 and 1995 were 14% and 15%, respectively. Thus, the percentage decline in 2007 again stands out as exceptional.

(iii) Consider partitioning the time series of September SIE into periods before and after a breakpoint T. Since there are 46 years in the time series, there are 45 possible breakpoints between years. For a given breakpoint T, find the minimum value of September SIE for the years before T (call it MIN), and the maximum value of September SIE for the years after T (call it MAX). Is it ever the case that MAX < MIN? The answer is yes, but only when T is between 2006 and 2007. That is the only breakpoint T in the time series for which all the values after T are less than all the values before T. This is illustrated in Figure 2 by the vertical and horizontal dotted lines. This indicates that the September SIE has never recovered from the jolt it received in 2007.

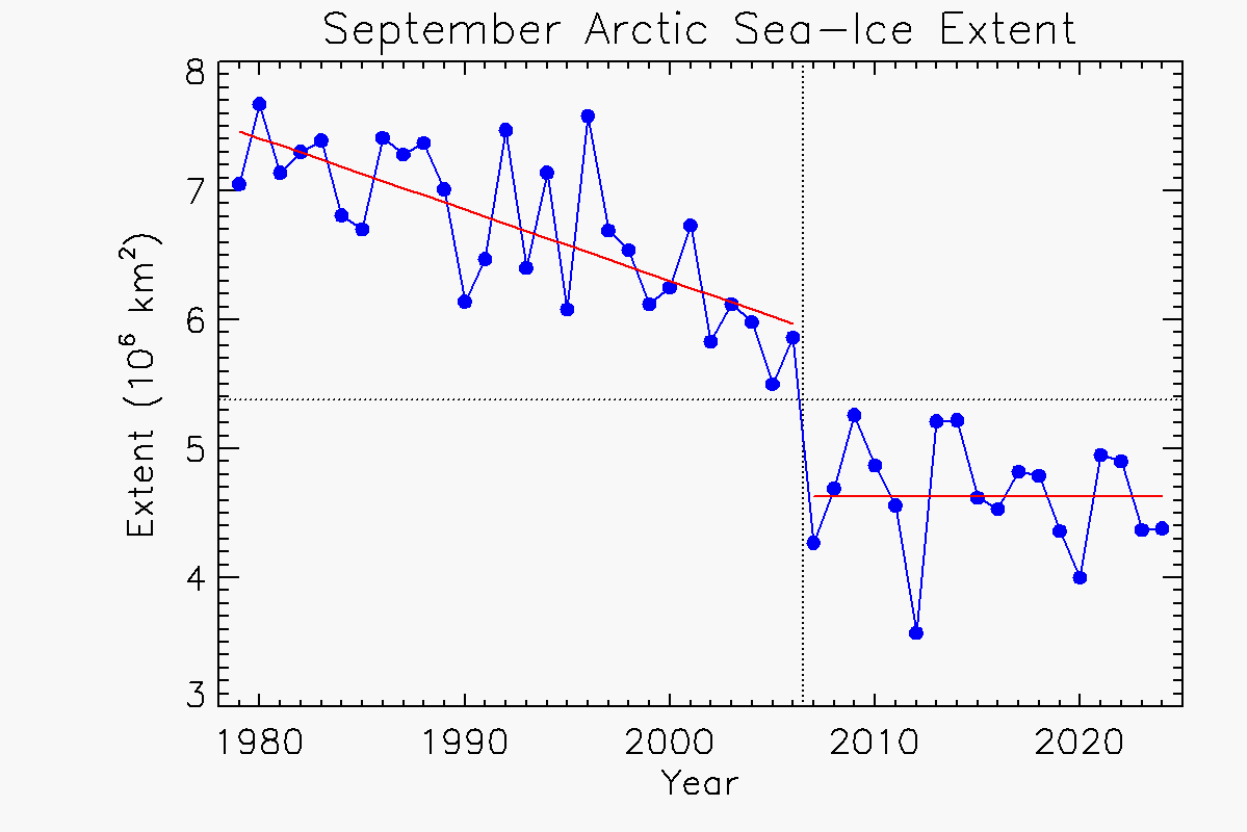

Figure 2. The same data as in Figure 1. The vertical dotted line between 2006 and 2007 marks the regime shift or breakpoint. The horizontal dotted line (at about 5.4×10^6 km^2) has the property that all the data values before the breakpoint are above the line and all the data values after the breakpoint are below the line. The only place in the time series where a horizontal line with that property can be drawn is for the breakpoint between 2006 and 2007. The linear least-squares fit for 1979-2006 is shown in red with slope -0.55×10^6 km^2 per decade. The mean sea-ice extent for 2007-2024 is also shown in red with value 4.63×10^6 km^2.

4. Detection of a regime shift

Rodionov (2004) presented an algorithm for detecting regime shifts in climate time series such as the Pacific Decadal Oscillation that have no long-term trend. The algorithm detects significant changes in the running mean of the time series using Student's t-test. The user must supply a parameter called the cut-off length, L, which is the minimum length of a regime. Although the algorithm is designed for time series with no long-term trend, Rodionov (2004) showed that it also works when a long-term trend is present (his Table 1). Sumata et al. (2023) used Rodionov's method for detecting a regime shift in sea-ice thickness, using a cut-off length of L = 7 years.

We first experimented with Rodionov's method on a time series of length 46 with values drawn from a normal distribution with zero mean and unit variance. We found that when the significance level of the t-test was set to p=0.05 the method detected spurious regime shifts for cut-off lengths $L \geq 7$, but when p=0.01 no such spurious regime shifts were detected. We therefore used p=0.01 in our application of the method to the September SIE time series.

We found that Rodionov's method detects a regime shift in the September SIE time series in 2007 for all values of the cut-off length L from 5 to 15 years. Additional regime shifts are also detected when $L \geq 9$ years. Note that in a time series with a long-term trend, as the cut-off length L increases, more and more of the running variability is in the trend as opposed to the fluctuations around the trend. For that reason, a shift in the running mean becomes more and more likely as L increases, which likely explains the additional regime shifts that are detected when $L \geq 9$ years.

Rodionov's method of regime shift detection depends on the significance level of the t-test and on the cut-off length L. It also assumes that the running variance of the time series, as calculated over segments of length L, does not change much over the entire time series. Although Rodionov's method does detect a regime shift in the September SIE in 2007, we would like to find a method that does not depend on tunable parameters and that tests the specific hypothesis of a regime shift in 2007 rather than searching for regime shifts in all possible years.

5. Bootstrap simulation

The full 46-year September SIE time series has a best-fit slope of $S_{46\text{-OBS}} = -0.78 \times 10^6$ km^2 per decade, and yet the last 18 years of the time series (2007-2024) has a best-fit slope of only $S_{18\text{-OBS}} = -0.099 \times 10^6$ km^2 per decade. Motivated by Figures 1 and 2 and the results of Sections 3 and 4, we want to determine how unusual that slope difference is. Specifically, we assume that the observed 46-year time series is well described by a linear model with slope $S_{46\text{-OBS}}$ plus residuals, and we ask how unusual it is for the final 18 years of that time series to have a best-fit slope of $S_{18\text{-OBS}}$. The null hypothesis (H_0) is that the observed slope $S_{18\text{-OBS}}$ is consistent with the 46-year linear model plus residuals. The alternative hypothesis (H_1) is that $S_{18\text{-OBS}}$ is not consistent with that model.

To test the hypotheses, we conduct a bootstrap simulation with the following general outline: Construct a large number of synthetic 46-year time series based on the same "linear model plus residuals" as the original time series; for each synthetic time series, calculate the slope of the final 18 years, creating a distribution of final 18-year slopes; compare the final 18-year slope of the original time series ($S_{18\text{-OBS}}$) to the distribution of synthetically derived slopes;

153 if $S_{18\text{-OBS}}$ lies in the outer 1% of the distribution, then reject H_0 and accept H_1; otherwise, do not
154 reject H_0.

155 The specific steps are as follows:

156 (i) Subtract the best-fit linear model of the 46-year September SIE time series (see Figure
157 1) from the time series itself to obtain residuals with zero mean.

158 (ii) Test whether the lag-1 autocorrelation of the residuals is significantly different from
159 zero or not, using the Durbin-Watson test (see Supporting Information, Text S1). The result is
160 that the lag-1 autocorrelation is not significantly different from zero, which means that the
161 bootstrap simulation does not need to account for autocorrelation in the residuals.

162 (iii) Randomly permute the order of the residuals and then add them back to the original
163 linear model to create a new (synthetic) time series. Calculate the best-fit slope for the full 46-
164 year synthetic time series (call it S_{46}) and the best-fit slope for the final 18 years (call it S_{18}).
165 Note that the slope S_{46} will be nearly the same as the slope of the original time series, but not
166 exactly the same, because the order of the residuals affects the least-squares fitting. For example,
167 a large anomaly near the middle of a time series has very little influence on the least-squares
168 slope, while the same anomaly at the end of the time series has a larger influence. For that
169 reason, S_{46} and S_{18} are both calculated and saved. Nevertheless, the synthetic time series has
170 nearly the same 46-year least-squares slope and residuals as the original time series. The real
171 quantity of interest is the slope of the final 18 years, S_{18}.

172 (iv) Repeat step (iii) 10,000 times to obtain a distribution of S_{18} and a distribution of S_{46}.
173 The resulting 10,000 pairs of numbers are plotted in Figure S1, with S_{18} on the X-axis and S_{46} on
174 the Y-axis.

175 The first point to note in Figure S1 is that the distribution of S_{46} is very narrow: its
176 standard deviation (0.057×10^6 km^2 per decade) is only 7% of the magnitude of its mean value
177 (0.78×10^6 km^2 per decade). This shows that most of the synthetic time series have nearly the
178 same least-squares slope as the original time series, and therefore nearly the same residuals (but
179 in a different order). Thus, the pool of 10,000 synthetic time series is representative of the
180 original time series for the purpose of the bootstrap simulation.

181 The second point to note in Figure S1 is that the observed value of the final 18-year slope
182 ($S_{18\text{-OBS}} = -0.099 \times 10^6$ km^2 per decade) is at the far extreme edge of the distribution of S_{18}: only
183 16 out of 10,000 values are larger than $S_{18\text{-OBS}}$. The standard deviation of S_{18} is 0.23×10^6 km^2
184 per decade, so $S_{18\text{-OBS}}$ exceeds the mean of S_{18} by 2.9 standard deviations. At the other end of the
185 distribution, only 13 out of 10,000 values are more than 2.9 standard deviations smaller than the
186 mean of S_{18}. Taken together, only 0.3% of the simulated slopes S_{18} are more extreme than the
187 observed value $S_{18\text{-OBS}}$. Therefore, we reject the null hypothesis and conclude that a linear model
188 is not appropriate for the 46-year time series of September SIE because the trend over the final
189 18 years is not consistent with such a model.

190

191 **6. Alternatives to the linear model**

192

193 In light of the results in the previous section, we consider several alternatives to a linear
194 model of September SIE: a piecewise-linear model with a breakpoint between 2006 and 2007, a
195 cubic polynomial, and a Gompertz model. Each alternative model contains four adjustable
196 parameters, so the models are directly comparable to one another. Since a linear model contains

only two adjustable parameters, the alternative models naturally provide better fits. A comparison of the models and their performance is given in Table 1.

The simplest piecewise-linear model of September SIE consists of a breakpoint between 2006 and 2007 and a linear fit on either side of the breakpoint. However, the slope of the best-fit line to the years 2007-2024 is $S_{18\text{-}OBS} = -0.099 \times 10^6$ km^2 per decade with standard deviation 0.20×10^6 km^2 per decade, which is statistically indistinguishable from zero, so a slope is unnecessary. The best-fit constant (in the least-squares sense) is the mean value, which is 4.6×10^6 km^2. The four parameters of the piecewise-linear model (shown in Figure 2) are then: the location of the breakpoint, the slope and intercept of the linear fit to the left of the breakpoint, and the constant fit (the mean) to the right of the breakpoint. This model is very simple to understand and interpret: September SIE declined approximately linearly for the first 28 years, then an unprecedented jolt hit in 2007 from which the SIE has never recovered. There has been no long-term trend since that time.

The cubic polynomial model (shown in Figure S2) is continuous – there is no breakpoint or jump in value. The idea is to see if a higher-order function can smoothly account for the large drop in September SIE in 2007, followed by a period of no long-term trend. One drawback of this model is the difficulty of explaining why the September SIE should evolve according to a cubic function of time.

The Gompertz function was invented to model human mortality and has been used to model the growth of animal populations, bacterial cells, and tumors (Gompertz function, 2024). It has also been used to model the September SIE (Stroeve et al., 2014; Hamilton, 2015). The Gompertz function has a sigmoid shape with slow growth (or decay) at the beginning and end, and faster growth (or decay) in the middle. The idea of using this model is to see if the faster

220 decay can be aligned with the drop in SIE in 2007, and the asymptotic value as $t \rightarrow \infty$ matched
221 with the mean SIE during 2007-2024. Details of the Gompertz model are in the Supporting
222 Information, Text S2 and Figure S2.

223 Of the three alternative models considered here, the one with a discontinuity in 2007
224 performs the best (Table 1). This lends further weight to the idea of a regime shift in 2007.

225

226

227

228 **Table 1.** Comparison of different models of the September sea-ice extent (SIE). The root-mean-
229 square (RMS) value of the residuals (fourth column) is in units of 10^6 km^2. The fraction of the
230 variance of the SIE that is explained by the model is given in the fifth column.

231

Model	**Continuous?**	**Number of parameters**	**RMS of residuals**	**Fraction of variance**
Linear	Yes	2	0.51	0.80
Piecewise-linear	No	4	0.41	0.87
Cubic	Yes	4	0.46	0.84
Gompertz	Yes	4	0.45	0.85

232

7. Discussion

We have shown that the September Arctic SIE underwent an abrupt, substantial, and persistent change in 2007, meeting the definition of a regime shift given by Reid et al. (2015). Before 2007, September SIE was declining approximately linearly. In September 2007, SIE had its largest year-to-year drop (by a wide margin) in the entire 46-year satellite record (1979-2024). Since 2007, September SIE has been approximately constant, i.e., no long-term trend.

The statistical evidence for a regime shift presented here calls for an explanation in terms of physical processes. While it is beyond the scope of the present work to conduct such process studies, e.g. with climate models, we can look to previous studies for insight. In the following, we consider the three segments of the September SIE time series: the decline (1979-2006), the extreme drop (2007), and the period of no long-term trend (2007-2024).

The decline of September SIE through 2006 was well documented at the time in observations and models (e.g., Lemke et al., 2007), although the models tended to underestimate the downward trend (Stroeve et al., 2007). More recently, Meehl et al. (2018) noted that the linear rate of decline of Arctic SIE was steeper during 2000-2014 than during 1979-1999. Their explanation is that "a combination of decadally varying tropical sea surface temperatures in the Pacific and Atlantic drove seasonally dependent patterns of stronger surface winds and sea ice drifts over the Arctic that produced accelerated decreases of Arctic sea ice concentrations after 2000." We note that their later period (2000-2014) spans the huge drop in September SIE in 2007 that initiated the regime shift, as well as the record-low September SIE in 2012. Their results are not inconsistent with ours because the trend in September SIE during 2000-2006 is about the same as during 1979-2000. Their steeper slope during 2000-2014 is due to the low values of SIE

from 2007 onward. In any case, the physical reason for the downward trend in Arctic SIE has been confidently attributed to global warming caused by anthropogenic greenhouse gas emissions (Fox-Kemper et al., 2021). Notz and Stroeve (2016) found that Arctic sea-ice loss is linearly related to anthropogenic CO_2 emissions.

The physical basis for a regime shift in 2007 is explained by Sumata et al. (2023) in reference to the sea-ice thickness: "The timing of the shift was preceded by a two-step reduction in residence time of sea ice in the Arctic Basin, initiated first in 2005 and followed by 2007." And then, "After the shift, the fraction of thick and deformed ice dropped by half and has not recovered to date." Similar conclusions about sea-ice loss were reached by Babb et al. (2023): the loss of multiyear ice (MYI) from the Arctic Ocean primarily occurred through stepwise reductions in 1989 and in 2006-2008; the reduction in 2006-2008 was the result of high MYI export and melt, and limited MYI replenishment. Maslanik et al. (2007) were the first to comment on the record-low SIE in 2007, also tying it to reduced MYI as well as ice transport: "Ice coverage in summer 2007 reached a record minimum, with ice extent declining by 42% compared to conditions in the 1980s. The much-reduced extent of the oldest and thickest ice, in combination with other factors such as ice transport that assist the ice-albedo feedback by exposing more open water, help explain this large and abrupt ice loss." The increase in the drift speed of Arctic sea ice (Rampal et al., 2009) also factored into the explanation given by Nghiem et al. (2007) for the significant reduction in perennial sea ice between March 2005 and March 2007. They found that a contributing mechanism was "ice loading into the Transpolar Drift (TD) together with an acceleration of the TD carrying excessive ice out of Fram Strait." For overviews of the 2007 SIE minimum, see Stroeve et al. (2008) and Zhang et al. (2008). The above observations clearly tie the record-low (at the time) SIE in September 2007 to the loss of MYI

279 through export. This led to a regime shift in the sea-ice thickness (Sumata et al., 2023) and (we
280 contend) a regime shift in the September SIE as well. In addition, Livina and Lenton (2013)
281 found an abrupt and persistent increase in the amplitude of the seasonal cycle of sea ice starting
282 in 2007, which they termed a tipping point. This is further evidence that 2007 was a pivotal year
283 for Arctic sea ice.

284 The period of no long-term trend in the September SIE (2007-2024) has been noted by
285 other researchers. Meier and Stroeve (2022) wrote: "The Arctic sea ice cover has undergone
286 substantial changes in the past 40+ years, including decline in areal extent in all months
287 (strongest during summer), thinning, loss of multiyear ice cover, earlier melt onset and ice
288 retreat, and later freeze-up and ice advance. In the past 10 years, these trends have been further
289 reinforced, though the trends (not statistically significant at $p<0.05$) in some parameters (e.g.,
290 extent) over the past decade are more moderate." In other words, they recognized that the trend
291 in Arctic SIE during approximately 2010-2020 was not significantly different from zero, but they
292 did not go so far as to call it a regime shift.

293 The fact that September Arctic SIE shows no trend during 2007-2024 may at first seem
294 hard to explain. The Earth continues to warm, and the Arctic is warming faster than the global
295 average (IPCC, 2021). One possibility is that the recent period of no trend is just interdecadal
296 variability. Baxter et al. (2019) found that "observational and model evidence shows that the
297 changes in summer sea ice since the 2000s reflect a continuous anthropogenically forced melting
298 masked by interdecadal variability of Arctic atmospheric circulation. This variation is partially
299 driven by teleconnections originating from sea surface temperature (SST) changes in the east-
300 central tropical Pacific" and this "has contributed to accelerated warming and Arctic sea ice loss
301 from 2007 to 2012, followed by slower declines in recent years, resulting in the appearance of a

slowdown over the past 11 years." In other words, they argue that the appearance of a slowdown in the decline of Arctic SIE since 2007 is due to interdecadal variability of Arctic atmospheric circulation.

As noted above, Sumata et al. (2023) found that after the regime shift of 2007, "the fraction of thick and deformed ice dropped by half and has not recovered to date." The variance of the sea-ice thickness also dropped abruptly in 2007 and has not recovered (their Figure 2), signaling the transition to a more uniform ice cover. With the Arctic Ocean thus dominated by first-year ice (confirmed also by Kwok, 2018), the SIE at the end of the summer melt season would be dominated by the production, melt, and export of first-year ice since the previous fall. Therefore, the September SIE during 2007-2024 may simply reflect the mean and year-to-year variability of first-year ice in a steady state (Figure 2). The Arctic Oscillation index, a climate index that characterizes the large-scale atmospheric circulation over the Arctic, has been in a positive phase since mid-2011 (NOAA Climate Prediction Center, 2024), which indicates lower than average air pressure over the Arctic (NOAA Climate.gov, 2024), driving a cyclonic circulation pattern in the Arctic Ocean with a lag of about one year (Morison et al., 2021). The persistence of this cyclonic mode in the ocean may be contributing to the steady state of the September SIE. This is similar to the argument made in the previous paragraph that the lack of trend in September SIE is due to interdecadal variability of Arctic atmospheric circulation.

Lindsay and Zhang (2005) proposed a three-stage framework for understanding the record or near-record lows in summer SIE in the years 2002-2005 that is partially applicable to 2007 and beyond. First, the sea ice was "pre-conditioned" through a gradual reduction in thickness during the late 1980s and 1990s. Second, a temporary change in atmospheric circulation embodied in two climate indexes, the Arctic Oscillation and the Pacific Decadal

Oscillation, provided the "trigger" that caused older, thicker sea ice to be flushed out the Arctic basin, resulting in an increase in the summer open water extent. Third, the positive ice-albedo feedback perpetuated and amplified the shift toward more summer open water and thinner ice. The feedback continued to drive the thinning of the sea ice even after the climate indexes returned to near-normal values in the late 1990s. The first and second stages of this framework apply equally well to the September SIE through 2007. The pre-conditioning stage was the thinning and areal reduction of 1979-2006. The trigger was the huge decline in 2007 caused by the export of ice from the Arctic basin. But annual declines have not been sustained (on average) in the post-2007 period, suggesting that the ice-albedo feedback has not been dominating the evolution of the ice cover.

Whatever the reason for the near-zero trend during 2007-2024, Arctic SIE is predicted to continue declining due to increasing global average air temperature caused by anthropogenic greenhouse gas emissions (Fox-Kemper et al., 2021). Based on global climate models, there is "*high confidence* that the Arctic Ocean will *likely* become practically sea ice free in the September mean for the first time … before the year 2050" in all emissions scenarios (Fox-Kemper et al., 2021). Thus, we would expect to see either a resumption of a steady decline in September SIE or a step-wise reduction through regime shifts facilitated by a younger and thinner ice pack that is more sensitive to external atmospheric forcing, whose decadal variability may also play a role.

Data availability

The data in Fetterer et al. (2017) are available from https://doi.org/10.7265/N5K072F8

An alternate URL is https://nsidc.org/data/g02135/versions/3

A direct link to September Arctic SIE data is:

https://noaadata.apps.nsidc.org/NOAA/G02135/north/monthly/data/N_09_extent_v3.0.csv

Acknowledgements

The author thanks Axel Schweiger, Ron Lindsay, and Jamie Morison for helpful comments and discussion. Funding was provided by NASA Interdisciplinary Research Grant 80NSSC20K1253.

References

Babb, D. G., Galley, R. J., Kirillov, S., Landy, J. C., Howell, S. E. L., Stroeve, J. C., et al. (2023). The stepwise reduction of multiyear sea ice area in the Arctic Ocean since 1980. *Journal of Geophysical Research: Oceans*,128, e2023JC020157. https://doi.org/10.1029/2023JC020157

Baxter, I., Q. Ding, A. Schweiger, M. L'Heureux, S. Baxter, T. Wang, Q. Zhang, K. Harnos, B. Markle, D. Topal, and J. Lu (2019). How Tropical Pacific Surface Cooling Contributed to Accelerated Sea Ice Melt from 2007 to 2012 as Ice Is Thinned by Anthropogenic Forcing, *Journal of Climate*, 32, 8583-8602, DOI: 10.1175/JCLI-D-18-0783.1

DiGirolamo, N., Parkinson, C. L., Cavalieri, D. J., Gloersen, P. & Zwally, H. J. (2022). Sea Ice Concentrations from Nimbus-7 SMMR and DMSP SSM/I-SSMIS Passive Microwave Data. (NSIDC-0051, Version 2). Boulder, Colorado USA. NASA National Snow and Ice Data Center Distributed Active Archive Center. https://doi.org/10.5067/MPYG15WAA4WX.

Fetterer, F., Knowles, K., Meier, W. N., Savoie, M. & Windnagel, A. K. (2017). Sea Ice Index. (G02135, Version 3). Boulder, Colorado USA. National Snow and Ice Data Center. https://doi.org/10.7265/N5K072F8. Date Accessed 11-10-2024.
Alternate URL: https://nsidc.org/data/g02135/versions/3

Fox-Kemper, B., H.T. Hewitt, C. Xiao, G. Aðalgeirsdóttir, S.S. Drijfhout, T.L. Edwards, N.R. Golledge, M. Hemer, R.E. Kopp, G. Krinner, A. Mix, D. Notz, S. Nowicki, I.S. Nurhati, L. Ruiz, J.-B. Sallée, A.B.A. Slangen, and Y. Yu (2021). Ocean, Cryosphere and Sea Level Change. In Climate Change 2021: The Physical Science Basis. Contribution of Working Group I to the Sixth Assessment Report of the Intergovernmental Panel on Climate Change [Masson-Delmotte, V., P. Zhai, A. Pirani, S.L. Connors, C. Péan, S. Berger, N. Caud, Y. Chen, L. Goldfarb, M.I. Gomis, M. Huang, K. Leitzell, E. Lonnoy, J.B.R. Matthews, T.K. Maycock, T. Waterfield, O. Yelekçi, R. Yu, and B. Zhou (eds.)]. Cambridge University Press, Cambridge, United Kingdom and New York, NY, USA, pp. 1211–1362, doi:10.1017/9781009157896.011.

Gompertz function (2024). Wikipedia, https://en.wikipedia.org/wiki/Gompertz_function
When accessed on 12/11/2024, this page was last edited on 8/13/2024 at 08:30 (UTC).

Hamilton, L. (2015). Pan-Arctic Outlook, contribution to the *Sea Ice Outlook: 2015 June Report*, Sea Ice Prediction Network, Arctic Research Consortium of the United States, https://www.arcus.org/sipn/sea-ice-outlook/2015/june

IPCC (2021). Summary for Policymakers. In: Climate Change 2021: The Physical Science Basis. Contribution of Working Group I to the Sixth Assessment Report of the Intergovernmental Panel on Climate Change [Masson-Delmotte, V., P. Zhai, A. Pirani, S. L. Connors, C. Péan, S. Berger, N. Caud, Y. Chen, L. Goldfarb, M. I. Gomis, M. Huang, K. Leitzell, E. Lonnoy, J. B. R. Matthews, T. K. Maycock, T. Waterfield, O. Yelekçi, R. Yu and B. Zhou (eds.)]. Cambridge University Press.

Kwok, R. (2018). Arctic sea ice thickness, volume, and multiyear ice coverage: losses and coupled variability (1958–2018), *Environ. Res. Lett.,* 13, 105005, https://doi.org/10.1088/1748-9326/aae3ec

Lemke, P., J. Ren, R.B. Alley, I. Allison, J. Carrasco, G. Flato, Y. Fujii, G. Kaser, P. Mote, R.H. Thomas and T. Zhang (2007). Observations: Changes in Snow, Ice and Frozen Ground. In: Climate Change 2007: The Physical Science Basis. Contribution of Working Group I to the Fourth Assessment Report of the Intergovernmental Panel on Climate Change [Solomon, S., D. Qin, M. Manning, Z. Chen, M. Marquis, K.B. Averyt, M. Tignor and H.L. Miller (eds.)]. Cambridge University Press, Cambridge, United Kingdom and New York, NY, USA.

414 Lindsay, R. W., and J. Zhang (2005). The Thinning of Arctic Sea Ice, 1988–2003: Have We
415 Passed a Tipping Point? *Journal of Climate*, 18, 4879-4894.
416
417 Livina, V. N., and T. M. Lenton (2013). A recent tipping point in the Arctic sea-ice cover: abrupt
418 and persistent increase in the seasonal cycle since 2007, *The Cryosphere*, 7, 275–286,
419 doi:10.5194/tc-7-275-2013
420
421 Maslanik, J. A., C. Fowler, J. Stroeve, S. Drobot, J. Zwally, D. Yi, and W. Emery (2007), A
422 younger, thinner Arctic ice cover: Increased potential for rapid, extensive sea-ice loss, *Geophys.*
423 *Res. Lett., 34,* L24501, doi:10.1029/2007GL032043.
424
425 Meehl, G. A., Chung, C. T. Y., Arblaster, J. M., Holland, M. M., & Bitz, C. M. (2018). Tropical
426 decadal variability and the rate of Arctic sea ice decrease. *Geophysical Research Letters*, 45,
427 11,326–11,333. https://doi.org/10.1029/2018GL079989
428
429 Meier, W.N., and J. Stroeve (2022). An updated assessment of the changing Arctic sea ice cover.
430 *Oceanography*, https://doi.org/10.5670/oceanog.2022.114.
431
432 Morison, J., R. Kwok, S. Dickinson, R. Andersen, C. Peralta-Ferriz, D. Morison, I. Rigor, S.
433 Dewey, and J. Guthrie (2021). The Cyclonic Mode of Arctic Ocean Circulation, *Journal of*
434 *Physical Oceanography*, 51, 1053-1075, DOI: 10.1175/JPO-D-20-0190.1
435

436 Nghiem, S. V., I. G. Rigor, D. K. Perovich, P. Clemente-Colon, J. W. Weatherly, and G. Neumann
437 (2007), Rapid reduction of Arctic perennial sea ice, *Geophys. Res. Lett.,* 34, L19504,
438 doi:10.1029/2007GL031138.
439
440 NOAA Climate.gov (2024). Climate Variability: Arctic Oscillation,
441 https://www.climate.gov/news-features/understanding-climate/climate-variability-arctic-
442 oscillation, accessed 12/24/2024.
443
444 NOAA Climate Prediction Center (2024). Standardized 3-Month Running Mean AO Index
445 Through November 2024,
446 https://www.cpc.ncep.noaa.gov/products/precip/CWlink/daily_ao_index/month_ao_index.shtml
447 Accessed 12/24/2024.
448
449 Notz, D. and J. Stroeve (2016). Observed Arctic sea-ice loss directly follows anthropogenic CO2
450 emission, *Science*, Vol 354, Issue 6313, pp. 747-750, DOI: 10.1126/science.aag2345
451
452 Rampal, P., J. Weiss, and D. Marsan (2009), Positive trend in the mean speed and deformation
453 rate of Arctic sea ice, 1979–2007, *J. Geophys. Res.,* 114, C05013, doi:10.1029/2008JC005066.
454
455 Reid, P.C., R.E. Hari, G. Beaugrand, D.M. Livingstone, C. Marty, D. Straile, J. Barichivich, E.
456 Goberville, R. Adriani, Y. Aono, R. Brown, J. Foster, P. Groisman, P. Helaouet, H. Hsu, R. Kirby,
457 J. Knight, A. Kraberg, J. Li, T-T Lo, R.A. Myneni, R.P. North, J.A. Pounds, T. Sparks, R. Stubi,

458 Y. Tian, K.H. Wiltshire, D. Xiao, and Z. Zhu (2015). Global impacts of the 1980s regime shift,
459 *Global Change Biology*, doi: 10.1111/gcb.13106
460
461 Rodionov, S.N. (2004). A sequential algorithm for testing climate regime shifts, *Geophysical*
462 *Research Letters*, 31, L09204, doi:10.1029/2004GL019448
463
464 Savin, N.E. and White, K.J. (1977). The Durbin-Watson Test for Serial Correlation with Extreme
465 Sample Sizes or Many Regressors. *Econometric*, 45, 1989-1996.
466 http://dx.doi.org/10.2307/1914122
467
468 Spreen, G., L. Kaleschke, and G.Heygster (2008). Sea ice remote sensing using AMSR-E 89
469 GHz channels, *J. Geophys. Res.*, 113, C02S03, doi:10.1029/2005JC003384.
470
471 Stroeve, J., M. M. Holland, W. Meier, T. Scambos, and M. Serreze (2007). Arctic sea ice
472 decline: Faster than forecast, *Geophys. Res. Lett.,* 34, L09501, doi:10.1029/2007GL029703.
473
474 Stroeve, J., M. Serreze, S. Drobot, S. Gearheard, M. Holland, J. Maslanik, W. Meier, and T.
475 Scambos (2008). Arctic Sea Ice Extent Plummets in 2007, *Eos Transactions*, Vol. 89, No. 2, pp.
476 13-20.
477
478 Stroeve, J., L. C. Hamilton, C. M. Bitz, and E. Blanchard-Wrigglesworth (2014). Predicting
479 September sea ice: Ensemble skill of the SEARCH Sea Ice Outlook 2008–2013, *Geophys. Res.*
480 *Lett.*, 41, 2411–2418, doi:10.1002/2014GL059388.

Sumata, Hiroshi, Laura de Steur, Dmitry V. Divine, Mats A. Granskog and Sebastian Gerland (2023). Regime shift in Arctic Ocean sea ice thickness, *Nature*, vol. 615, 443-449 https://doi.org/10.1038/s41586-022-05686-x

Zhang, J., R. Lindsay, M. Steele, and A. Schweiger (2008). What drove the dramatic retreat of arctic sea ice during summer 2007?, *Geophys. Res. Lett.,* 35, L11505, doi:10.1029/2008GL034005.

Geophysical Research Letters

Supporting Information for

Regime Shift in Arctic Ocean Sea-Ice Extent

Harry L. Stern[1]

[1]Polar Science Center, Applied Physics Laboratory, University of Washington, Seattle

Contents of this file

Text S1 and Text S2

Figure S1 and Figure S2

Introduction

Text S1 and Figure S1 are referenced in Section 5 of the main text.

Text S2 and Figure S2 are referenced in Section 6 of the main text.

Text S1. Durbin-Watson test

Figure 1 (main text) shows the time series of September Arctic SIE (blue dots) and the best-fit linear model (red line). Subtracting the SIE from the linear model leaves a time series of residuals. In Section 5, we stated that the lag-1 autocorrelation of the residuals is not significantly different from zero. That result comes from applying the Durbin-Watson test, which specifically tests whether the residuals from ordinary least-squares regression are autocorrelated or not (Savin and White, 1977).

Let the residuals be denoted by r_j for j=1 to n where n=46 in our case. The test statistic is

$$d = \frac{\sum_{j=2}^{n}(r_j - r_{j-1})^2}{\sum_{j=1}^{n} r_j^2}$$

which is approximately 2(1−ρ) where ρ is the lag-1 autocorrelation. The test statistic d can have values between 0 and 4. A value of d = 2 means there is no autocorrelation. A value substantially below 2 means the data are positively autocorrelated. A value substantially above 2 means the data are negatively autocorrelated.

The test statistic is compared to values in the Durbin-Watson tables (see Savin and White (1977) for tables). For the significance levels α = 0.01 and α = 0.05, and the sample size n, and the number of regressors k (excluding the intercept term), the tables give lower and upper critical values, denoted by dL and dU.

The null hypothesis is that the autocorrelation is indistinguishable from zero. To test the alternative hypothesis that the autocorrelation is positive:

If d < dL then reject the null hypothesis and accept that the autocorrelation is positive.

If d > dU then do not reject the null hypothesis.

If dL < d < dU then the test is inconclusive.

The tables have rows for sample sizes 45 and 50 but not for 46. The user is instructed to use the next lowest sample size, namely n=45 in our case. The number of regressors (excluding the

intercept term) is k=1 (i.e., the slope of the regression line). The lower and upper critical values from the tables are:

For $\alpha = 0.01$, dL = 1.288 and dU = 1.376

For $\alpha = 0.05$, dL = 1.475 and dU = 1.566

In our case, the test statistic is $d = 1.668$, so we do not reject the null hypothesis even for the less stringent value of α. In other words, the lag-1 autocorrelation of the residuals (which is 0.148 in our case) is not significantly different from zero.

Text S2. Gompertz model

The Gompertz function is given by $f(t) = a * \exp(-b * \exp(-ct))$ where t is time and a, b, c are parameters. At t=0, $f(0) = a * \exp(-b)$ which is very close to zero when b is large. In the limit as t goes to infinity, $f(t)$ approaches a. By choosing $a < 0$ and b large, the function $f(t)$ decays from 0 to a. By adding a constant to $f(t)$ we can make it fit the September SIE time series:

$$f(t) = f_0 + a * \exp(-b * \exp(-ct))$$

where t is measured in years, t=0 corresponds to 1979, and t=45 corresponds to 2024. The constant f_0 is approximately equal to the September SIE in 1979, in units of 10^6 km^2. The constant a is approximately equal to the change in September SIE from 1979 to 2024, in units of 10^6 km^2. As an initial approximation, we set $f_0 = 7.1$ and $a = -2.5$ so that as $t \rightarrow \infty$, $f(t) \rightarrow f_0 + a = 7.1 + (-2.5) = 4.6$, which is equal to the mean September SIE during 2007-2024.

The constant c should be chosen such that $\exp(-ct)$ is small when t=45 (year 2024). With c = 0.15 we have $\exp(-0.15*45) = 0.001$, which is sufficiently small.

The growth rate (or decay rate) of the Gompertz model is df/dt, so the time of maximum decay rate can be found by solving $d^2f/dt^2 = 0$ for t. The result is $t_{max} = \ln(b)/c$. If we want t_{max} to correspond to the year 2007 or earlier, then $t_{max} \leq 28$ so $\ln(b) \leq 28 * 0.15 = 4.2$ or $b \leq 67$. We select $b = 40$ as an initial guess.

Now that we have initial estimates of all four parameters, we can use an iterative method to find the parameter values that minimize the root-mean-square (RMS) difference between the September SIE and the Gompertz model (i.e., the residuals). The result is: $f_0 = 7.1$, $a = -2.7$, $b = 33$, $c = 0.16$, yielding a Gompertz model with RMS residual 0.45×10^6 km^2 (Table 1). The Gompertz model is shown in Figure S2.

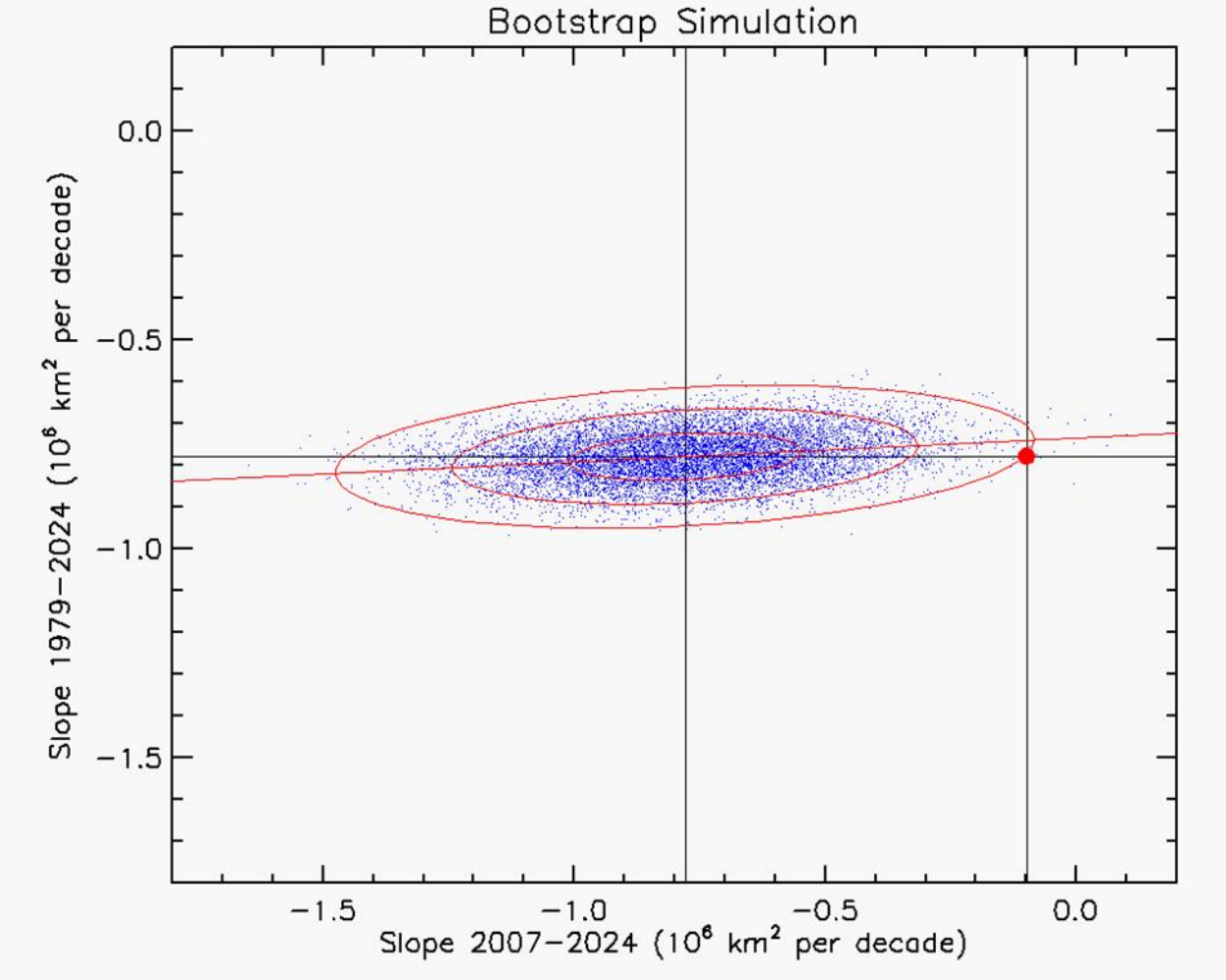

Figure S1. Result of the bootstrap simulation with 10,000 realizations (blue dots). The X-axis is the slope of the best-fit line to the final 18 years of the synthetic time series (S_{18}). The Y-axis is the slope of the best-fit line to the full 46-year synthetic time series (S_{46}). The red dot marks the values for the observed September sea-ice extent: X = -0.099×10^6 km^2 per decade for the final 18-year slope, and Y = -0.78×10^6 km^2 per decade for the full 46-year slope. The red ellipses are 1, 2, and 3 standard deviations from the mean of the distributions. The ellipses are slightly tilted because a relatively large (or small) value of S_{46} tends to be accompanied by a relatively large (or small) value of S_{18}. Notice that the red dot is at the far extreme edge of the distribution of S_{18},

indicating that the slope of the final 18 years of the observed September sea-ice extent is not consistent with a linear model of the full 46-year September sea-ice extent.

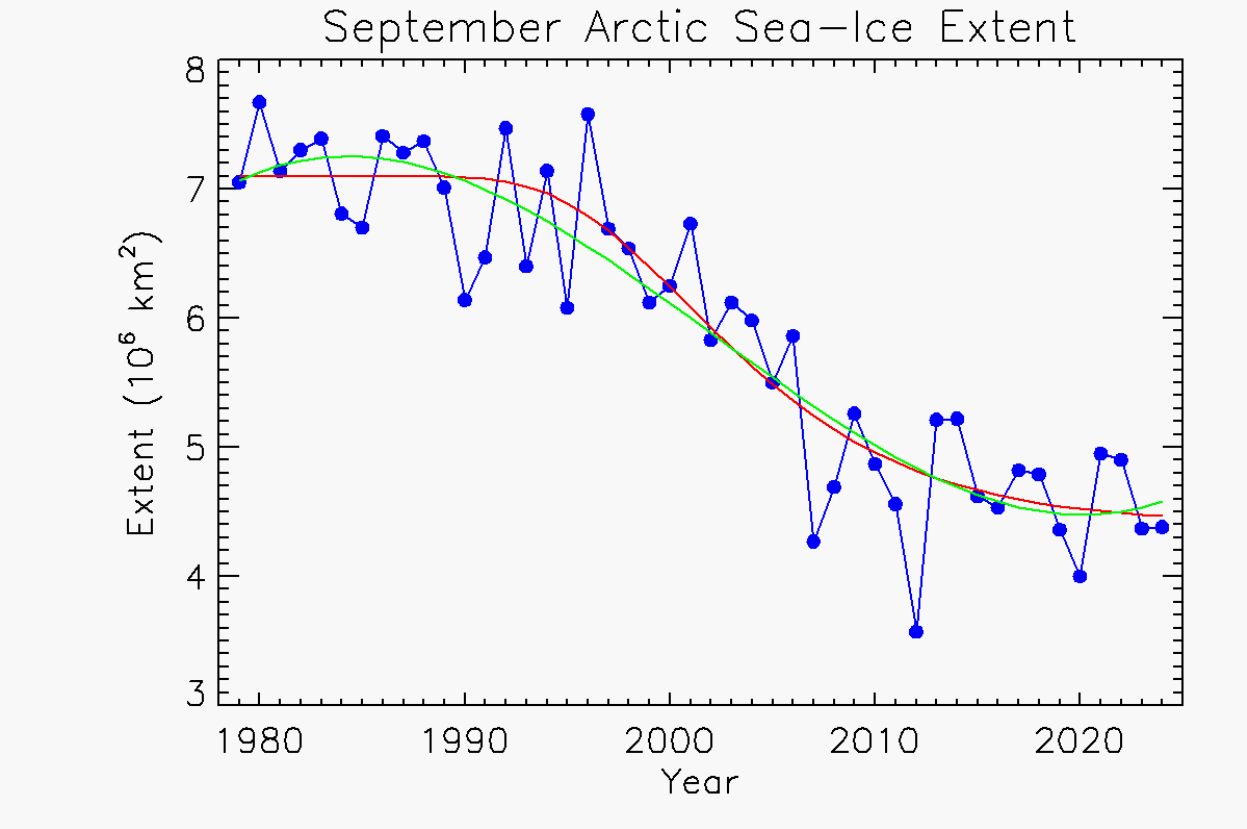

Figure S2. September Arctic sea-ice extent (blue dots, in units of 10^6 km^2) from the NSIDC Sea Ice Index (Fetterer et al., 2017). The best-fit Gompertz function is shown in red, and the best-fit cubic polynomial is shown in green.